

## Power2009-81019

### IDENTIFICATION OF ABNORMAL ROTOR DYNAMIC STIFFNESS USING MEASURED VIBRATION INFORMATION AND ANALYTICAL MODELING

Ned M. Endres, Principal MDS Specialist

RoMaDyn Corporation

#### ABSTRACT

It is a relatively common practice to address the problem of unacceptable synchronous (1X) vibration levels (like unbalance) by applying corrective balance weights after a thorough review of vibration measurements, available engineering information, and prior balancing history of a unit if available. The balance history might include balance plane weight maps and/or balancing influence data. On occasion, other vibration malfunctions and symptoms within measured vibration data, such as misalignment, a rub, or proximity probe journal target area slow roll (sometimes called “runout” or “glitch”) can also appear to be “unbalance” but are not. A principal requirement when performing any corrective balancing of a rotor is that the fundamental synchronous rotor response of the unit should always be linear and time invariant. The fundamental synchronous rotor response is directly proportional to dynamic forces and inversely proportional to dynamic stiffness. If the principle requirements cannot be met while balancing, any further balancing of the rotor should be terminated and other root causes for the unacceptable synchronous vibration levels should be investigated.

This paper will discuss a case history involving a steam turbine generator unit where excessive synchronous vibration levels were measured at the LP turbine bearings during transient and steady state operation. The initial concern was a steady increase in vibration levels at the LP turbine under steady state conditions. Prior balancing history and balancing information was reviewed and initial corrective balancing was performed. Initial correction of the unbalance proved to be inadequate, and the unit exhibited a significant change in balance influence. Since the response of the rotor to balance correction was not predictable and inconsistent with prior balancing data, alternative root causes for the unbalance symptoms were investigated. Integration of measured vibration data and

numerical modeling were essential with proper identification of the root cause of the unbalance symptoms.

#### INTRODUCTION

RoMaDyn was retained by plant management to provide vibration diagnostics expertise to analyze elevated vibration levels of their 45 MW steam turbine generator. The unit was seeing vibration levels of 4-5 mils pp at LP turbine bearing #4, with levels of 10 mils pp while passing through the first balance resonance during startups and shutdowns. This vibration data and other anecdotal information suggested that field balancing might reduce synchronous vibration levels. Initial field balancing results indicated that the LP turbine rotor sensitivity to unbalance had changed compared to successful field balancing measurements from 1992. Subsequent analytical modeling of the unit and outage inspections revealed that the LP turbine rotor had a radial shaft crack between bearing #3 and the last LP turbine exhaust stage.

The economic impact of the potential cracked shaft failure while in service was estimated as \$4,930,000 (\$6,900,000 in 2008 dollars). By correctly identifying this shaft crack before catastrophic failure, this cost was avoided.

#### INSTRUMENTATION

Proper vibration instrumentation is essential for obtaining accurate vibration data and proper machinery protection. This 45MW steam turbine generator unit was equipped with Bently Nevada 3300 proximity probes and proximitors at each bearing. These probes are reporting directly to a Bently Nevada 3500 vibration monitoring/protection system located in an adjacent turbine control room. Proximity transducers are installed in an X-Y orthogonal configuration at each turbine and generator bearing at 45 degrees left and right of top dead center, TDC,

(45L and 45R) for each of the four bearings. The system is also equipped with a Keyphasor® probe located at 0 degrees left of TDC to provide a once-per-turn reference for speed reference and diagnostic purposes.

This 45 MW steam turbine was driving a 2-pole 3600 rpm generator. As shown on the Machinery Arrangement Sketch (figure 1), the unit was equipped with X-Y shaft-relative proximity probes on all bearings. The unit was also equipped with a thrust probe at turbine bearing #1.

Throughout this paper, Bently Nevada naming conventions for probe orientations will be used. The Y proximity probe (45L) will be referred to as the “vertical” probe and the X proximity probe (45R) will be referred to as the “horizontal” probe, as viewing the unit from the turbine thrust bearing towards the generator non-driven end bearing, see figure 1 below.

All vibration monitors appeared to be functioning correctly throughout the measurements except for the differential expansion monitor that stayed in alarm during all machine conditions. It was suspected that this monitor/transducer system may not have been configured correctly.

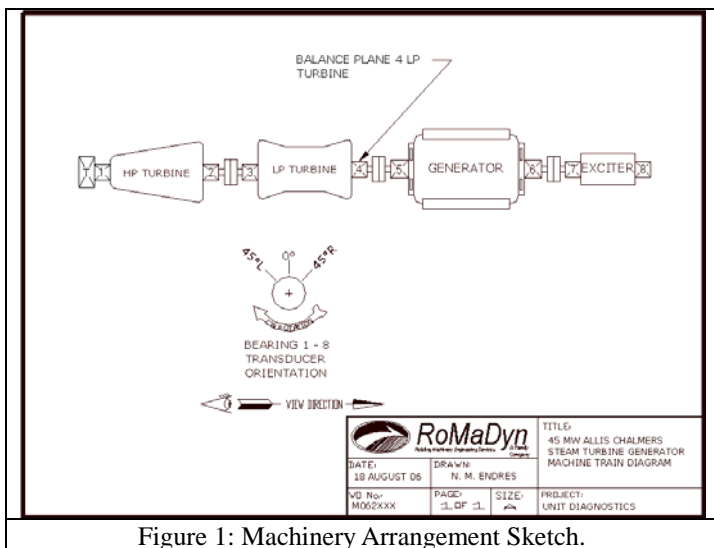


Figure 1: Machinery Arrangement Sketch.

For the onsite balancing, all vibration probe signals were field wired from the monitoring system to a Bently Nevada ADRE® 208 DAIU to acquire diagnostic data. Prior to arriving onsite, RoMaDyn personnel were requested to review and analyze vibration data collected in early August 2006 by plant personnel. The original diagnose was that field trim balancing should be implemented to improve vibration conditions. Vibration levels steadily increased and reach 5 mils pp just prior to a forced shutdown on 13 August due to high vibration levels. The unit could not be restarted. Subsequently, RoMaDyn was brought to site to perform trim balancing.

## INITIAL MEASUREMENTS AND OBSERVATIONS

An initial field balance and vibration analysis was performed on an Allis Chalmers 45 MW steam turbine generator from 21 to 25 August 2006. As mentioned previously, initial data acquired by the plant personnel covering the period from 1 to 13 August 2006 was forwarded to offsite RoMaDyn personnel for analysis and recommendations. This data indicated that the unit was operating at between 4-5 mil pp at bearing #4, and approaching 10-mil pp during startup and shutdown as the LP Turbine rotor passed through its first balance response region from 1000 to 1600 rpm. The data showed clear evidence of unbalance. Upon RoMaDyn traveling to site, an attempt to field balance the LP turbine was made on 23 August 2006. Initially, the unbalance state was severe enough that the unit could not pass through its first balance resonance and remain below 10-mil pp at bearing #4, see figure 2.

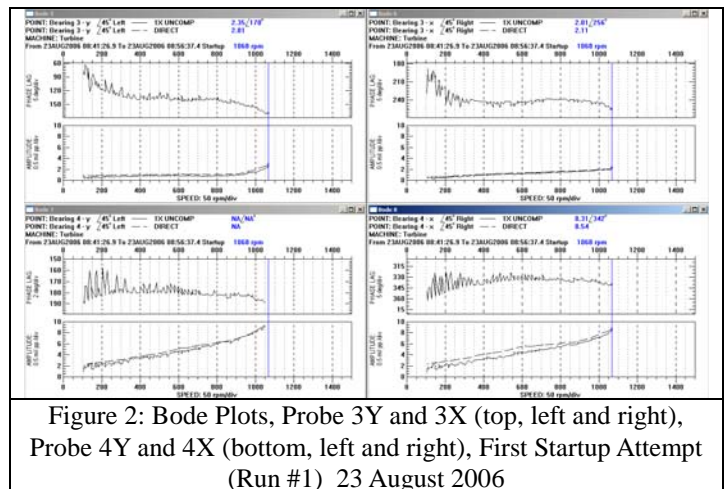


Figure 2: Bode Plots, Probe 3Y and 3X (top, left and right), Probe 4Y and 4X (bottom, left and right), First Startup Attempt (Run #1) 23 August 2006

Based on the vibration data to 1068 rpm, a balance weight correction was added to #4 bearing balance plane (LP turbine) of 260 grams @ 105° (against rotation from the 4X probe; balance hole #21). This correction weight allowed the unit to pass through its first balance resonance. At 2880 rpm, the unit was returned to turning gear due to the rapid rise in the 1X synchronous vibration; see Figure 3 and the weight plane map in sketch 1.

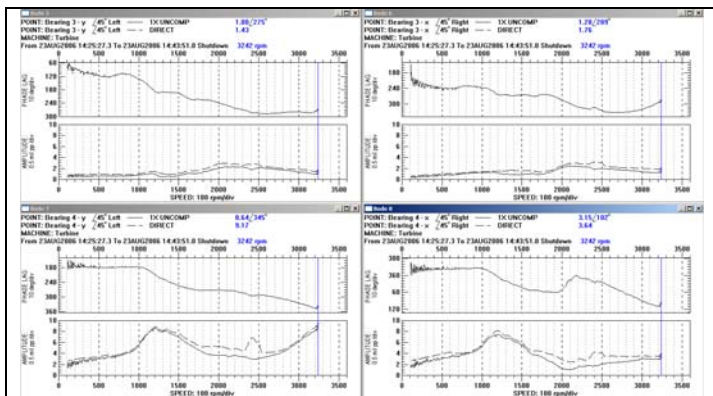
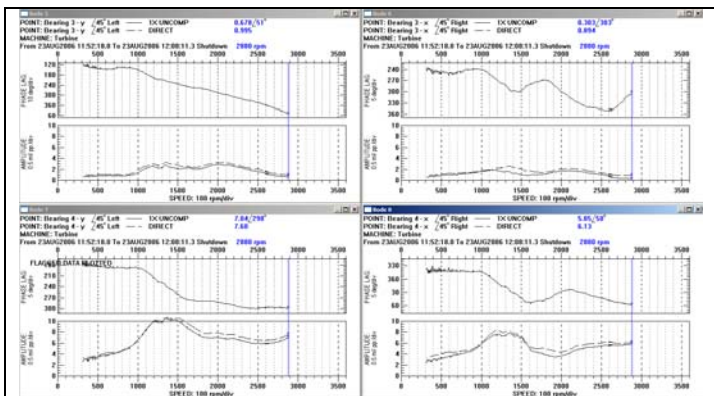
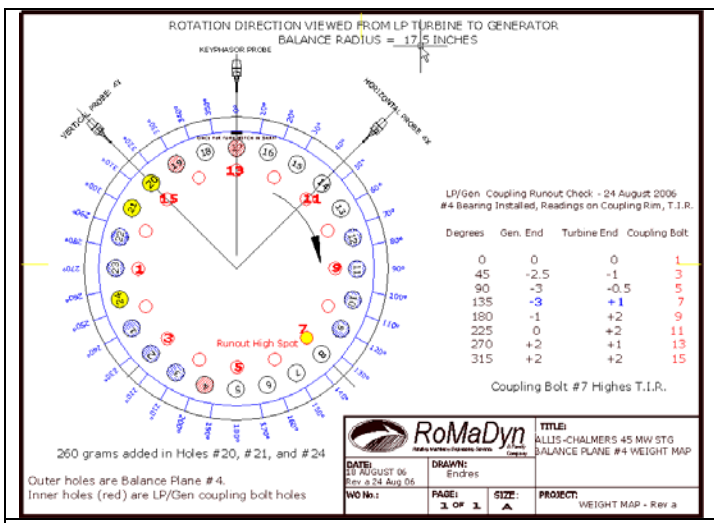


Figure 3: Bode Plots, Probe 3Y and 3X (top, left and right), Probe 4Y and 4X (bottom, left and right), Second Startup Attempt (First Balance Correction, Run #2) 23 August 2006 260 grams @ 105°

Figure 4: Bode Plots, Probe 3Y and 3X (top, left and right), Probe 4Y and 4X (bottom, left and right), Third Startup Attempt (Second Balance Correction, Run #3), 23 August 2006, Additional 260 grams @ 90° and 260 grams @ 150°



Sketch 1: Weight Plane Map After Balancing Attempt

A second balance correction was made by adding an additional 260 grams @ 90° (balance hole #20) and 260 grams @ 150° (balance hole #24). With the three weights added from both Runs #1 and #2, the net combined effect was 704.69 grams @ 115°; between balance holes #21 and #22, see figure 4 and the weight plane map.

This additional balance weight allowed the unit to be brought up to 3220 rpm before probe 4Y exceeded 10 mil pp. The response through the first balance resonance had been reduced from 10-mil pp (Run #2, Probe 4Y) to approximately 6.5 mil @ 1250 rpm (Run #3, Probe 4Y). Although the unit was responding positively to correction weights, its behavior was significantly different when compared to previous balance corrections (April 1992). In 1992, approximately 70 grams was required to reduce the synchronous 1X vibration by 1 mil pp. On 23 August 2006, it was taking approximately 140 grams to reduce the 1X vibration by 1 mil pp. One of the assumptions in balancing is linearity and repeatability, i.e. the system's response to corrective balancing does not change with time for a given set of operating conditions. Clearly, from April 1992 when the LP turbine rotor was successfully field balanced to 23 August 2006, the sensitivity of the LP turbine rotor had decreased, i.e. twice as much weight was required in 2006 for the same effect that was observed in 1992.

Since vibration is the summation of forces divided by dynamic stiffness, one can conclude that the LP turbine rotor / bearing system has stiffened, i.e. more centrifugal force (due to addition of balance weights) is required to get the same amount of change in synchronous 1X vibration. One of the possibilities is mis-alignment (offset) between the generator and LP turbine rotors. With a generator rotor weighing 46,000 lb and a LP turbine rotor weighing 23,000 lb, turbine to generator shaft mis-alignment will tend to have a greater effect on the LP turbine rotor.

A runout check of the LP Turbine / Generator Coupling was made on August 24. The measured runout indicated that the coupling (shaft) centerlines were not within the 1 mil offset tolerance. Maximum T.I.R. of 3-4 mils was indicated at coupling bolt #7, which was in line with the unbalance location, see weight plane map above. After reviewing runout measurements for bearing #4 from 1992, there was no evidence

of significant change in runout. This indicated the mechanical bow of the rotor was not responsible to the observed unbalance change.

One significant indication that rotor stiffness had been affected was the change in slow roll behavior at 350 rpm while lift oil was switched on and off. In general, at rotor speed equal to and below 10% of operating speed (3600 rpm), vibration levels should be due to electrical (residual magnetism, noise ...) and/or mechanical slow roll or “glitch” at the proximity probe target area. With the lift oil switched on, the shaft average centerline positions at both bearings #3 and #4 rose. Shaft relative orbits clearly showed dynamic motion at 350 rpm. The indicated “heavy spot” at bearings #3 and #4 were in good agreement with the polar plot data from the balancing attempts, see figure 5, top. When the lift oil was turned off at 350 rpm, the rotor moved downward approximately 3 mils at bearing #3 and 2 mils at bearing #4. At 350 rpm, the apparent dynamic motion at bearing #3 was much higher with the lift oil switched on. This observed effect of the rotor being lifted more at bearing #3 and increased rotor static deflection was possibly due to opening of the suspected shaft crack. When the lift oil was switched off, rotor motion was downward, dynamic motion decreased due to a reduction in static deflection, and the suspected crack at bearing #3 partially closed (figure 5, bottom). By floating the rotor while on lift oil, shaft crack was opened and resulted in increased deflections. The above behavior suggests that a possible cracked shaft somewhere in the LP turbine rotor might be responsible for observed behavior.

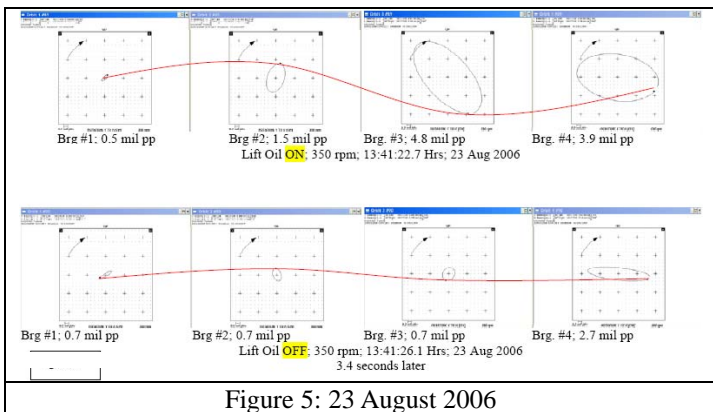


Figure 5: 23 August 2006

At 1210 rpm (first balance resonance) on 23 August 2006, the rotor deflection shape looked essentially the same as it did at 350 rpm when the lift oils was switched off, see figure 5 bottom plot, with the majority of the motion being at bearing #4 in the horizontal plane. By comparing the deflection shapes on 13 August 2006 to those of 23 August 2006, very little change was observed at bearings #1 and #2. However, the phase angle of the high spot in orbit of bearing #3 had changed 180 degrees, and the orbit motion at bearing #4 had shifted from being mostly vertical to primarily horizontal, see figure 6. Again, this type of behavior tended to suggest that a possible cracked shaft

somewhere in the LP turbine rotor might be responsible for observed vibration characteristics.

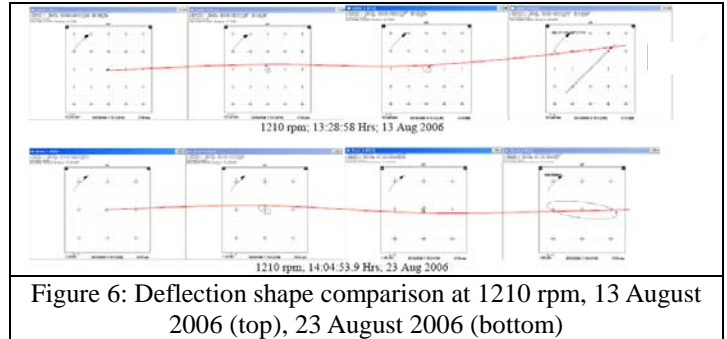


Figure 6: Deflection shape comparison at 1210 rpm, 13 August 2006 (top), 23 August 2006 (bottom)

### INSPECTION OF LP TURBINE ROTOR

Since the vibration data and results of initial balancing of the turbine suggested that a potential shaft crack might be present, the unit was taken offline for an inspection. On 25 August the decision was made to completely disassembly the LP turbine and generator for inspection. These rotors were removed and shipped to an outside repair facility for inspection and repair. NDE inspections consisted of boreside visual examination, wet fluorescent magnetic particle testing, and ultrasonic testing. The inspection of LP turbine rotor revealed a 260-270 degree circumferential crack on the #3 bearing end of the LP rotor. The crack was located between the gland seals and last stage wheel, photo 1 and photo 2.



Photo 1: Prior to leaving plant

The appearance of the crack near bearing #3 gland seal posed a significant question. Why were the 1X synchronous vibrations higher at bearing #4 when the rotor crack was near bearing #3? The answer was not immediately obvious. Therefore, RoMaDyn was requested to perform an analytical analysis of the rotor system and investigate (compute) the effects of potential rotor cracks near bearing #3 on rotor mode shapes and balance response.



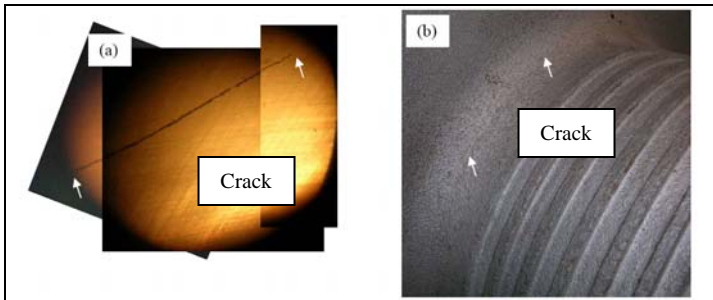


Photo2: a) Bore surface connected circumferential crack, about 1.5 inches long and spanning 51 degrees, b) Outside circumferential linear crack about 21 inches long and spanning 260 degrees.

## ANALYTICAL MODELING OF UNIT

### Overview

An analytical rotor model of the unit was created in order to evaluate the most likely location of the residual unbalance in the rotor system. The rotor-modeling program is a forced response program based on simple finite element methodology. It calculates the motion of a mechanical system produced by the applied forces. The program allows several variables to be selected as the independent variable for calculation. The most commonly selected is perturbation speed, which produces data equivalent to a normal transient startup or shutdown. In addition to the forced response calculations, the program contains optimization algorithms to determine the values of machinery parameters including the unbalance force distribution. The unbalance force distribution is determined by comparing calculated vibration displacement from the rotor model with actually measured 1X displacement values imported from a vibration response database (an ADRE® database in this case). The unbalance force distribution is modified until the calculated 1X vibration matches the measured 1X values.

### Model Development

A rotor dynamics analysis model facilitates modeling of rotor-bearing system, performing a damped-unbalance response analysis, calculating and viewing response results at rotor locations where it cannot be measured, determining “critical” speeds, determining possible effects of unbalance, and estimating the unbalance distribution and bearing stiffnesses of an existing unit from measured vibration data. The two approaches for conducting an analysis are to calculate results from initial engineering guess of critical system parameters (like bearing stiffness...) or to use measured vibration data (from and ADRE® database to compute results. The measured data can also be used to refine the original engineering parameter estimates yielding better analysis results.

The initial step of constructing a rotor is to get a geometric description of the rotor, through either engineering blue prints or measurements. Using the rotor geometry, a model of the turbine and generator rotors are constructed one shaft element at a time. At least one shaft element is inserted into the model for each change in shaft diameter. Disk elements can also be added to model blade stages and other masses. In addition to rotor elements, bearing elements are included at the journal locations. The effects of bearing stiffness and damping are specified for each bearing element. At least one bearing element must be added at each journal location. Tapered or curved rotor sections are modeled by dividing the section into a series of elements with the diameter of each element equal to the average diameter of that part of the taper. The influence of the housing (stiffness, damping...) can be included by housing elements, see figure 5. All relevant model parameters (like shaft material modulus, bearing stiffness...) are also added to the analytical model.

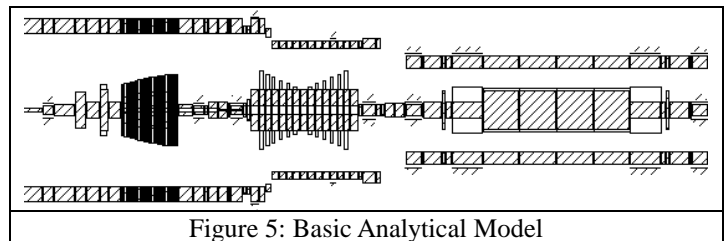


Figure 5: Basic Analytical Model

Proximity probe (P) points are inserted into the model at locations where measured vibration data is available (and imported into the model) or at locations where shaft relative deflections are to be calculated. Unbalance (U) can be included at prescribed points and circumferential angles. A once-per-revolution speed reference (K) point can also be included, see figure 6.

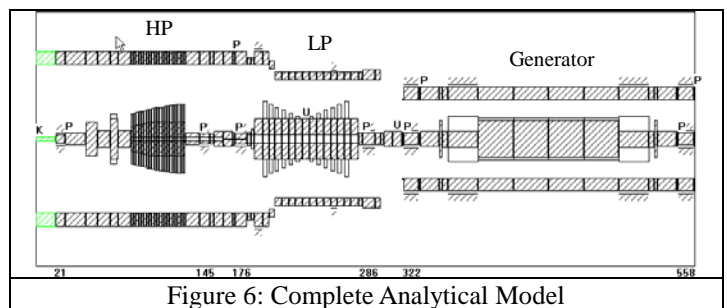
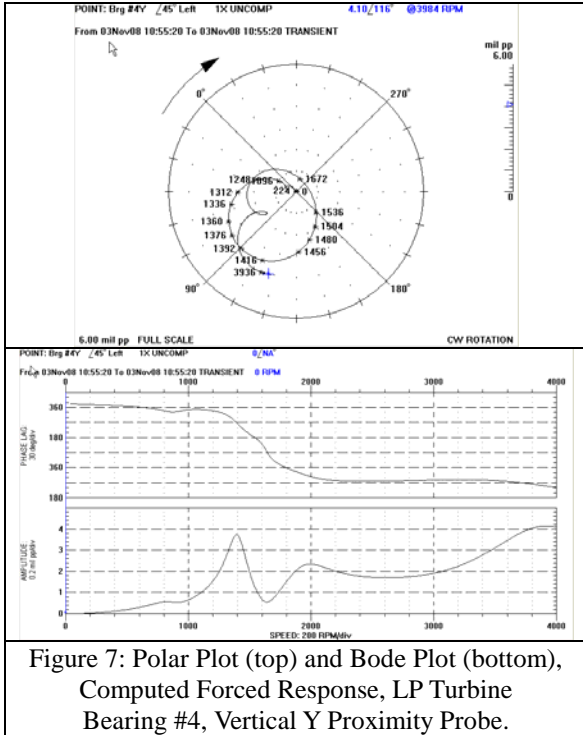


Figure 6: Complete Analytical Model

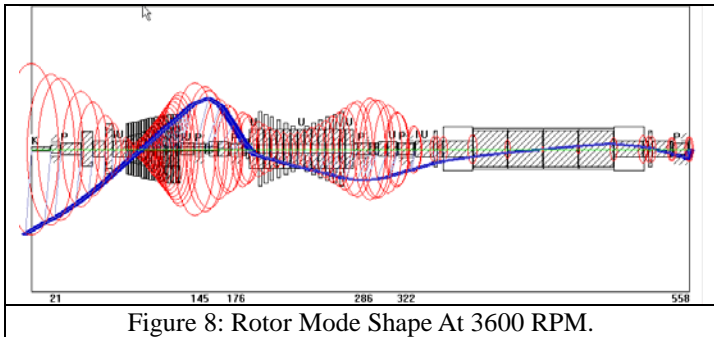
With a completed model, rotor forced response can be calculated over a desired speed range, see figures 7 and 8. If vibration data is available, it can be imported into the model and used to compute the unbalance distribution for the rotor and/or refined bearing parameters, like bearing stiffness and damping properties.



Unbalance Distribution	Apr. 1992	1 Aug. 06	2 Aug. 06
Angles Measured Against Rotation	lb-in @ deg. From TDC	lb-in @ deg. From TDC	lb-in @ deg. From TDC
Bearing #1	5 @ 72	1 @ 269	0.6 @ 335
Bearing #2	6 @ 247	1 @ 57	1 @ 0
Bearing #3	21 @ 65	31 @ 212	27 @ 208
LP Turbine Mid Span	21 @ 69	20 @ 58	20 @ 50
Bearing #4	6 @ 343	4 @ 58	6 @ 52
LP/Gen. Coupling	<b>9 @ 137</b>	42 @ 218	<b>37 @ 215</b>
Bearing #4		26 @ 19	23 @ 15

Table 1: Computed Unbalance Distribution

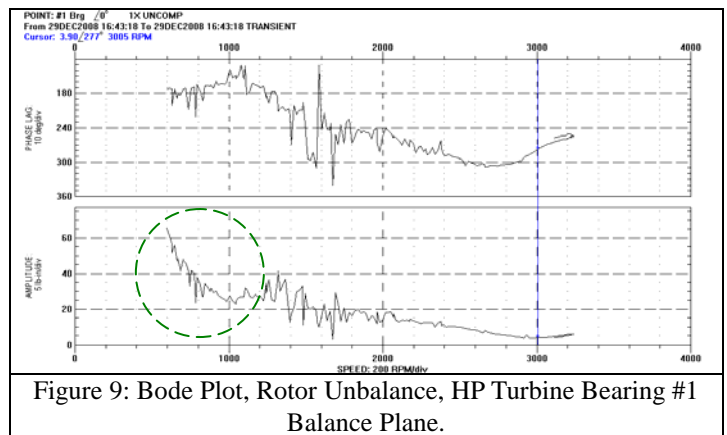
Based upon vibration measurements and rotor model computations, residual unbalance at the LP / Generator Coupling on 2 August 2006 was estimated to be 37 lb-in @ 215°. By comparison, the combined effect of the three weights added during balance runs #2 and #3 on 23 August, had an equivalent effect of 27.2 lb-in. Again, these computed results were consistent with the field balancing data findings; the weight added in run #2 and #3 were in the right location, but were not of sufficient magnitude. The nonlinear nature of the crack appeared to have a profound effect leading to the observed balance weight difference.



Plots of unbalance vs. rpm for the third run on August 23 are depicted in figures 9 through 15. As the rotor mode shape is constantly changing as a function of operating speed, so does its “effective” mass distribution, i.e. unbalance. This is clearly seen in these data plots and as one would expect, at higher speeds, the effective unbalance is less (multi-mode vs. one lumped mode).

### AUGUST 2006 VIBRATION ANALYSIS

Vibration data acquired from April 1992, 1 August 2006, 2 August 2006, and 23 August 2006 via an ADRE® data acquisition system was processed through the rotor-modeling program in order to determine the unbalance distributions (balance influence) and any potential changes in unbalance distribution. An initial check of the rotor model was performed by examining the computed unbalance distribution versus the initial balance corrections performed on 23 August. Table 1 shows computed unbalance distribution for three dates; April 1992, August 1<sup>st</sup> and August 2<sup>nd</sup>.



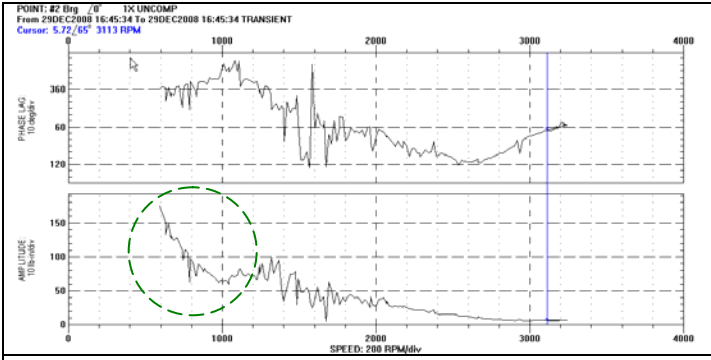


Figure 10: Bode Plot, Rotor Unbalance, HP Turbine Bearing #2 Balance Plane.

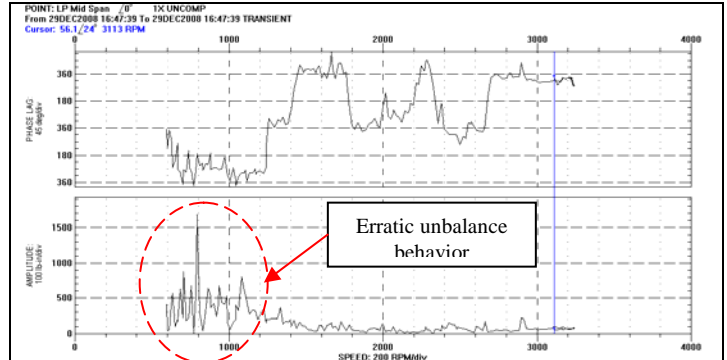


Figure 12: Bode Plot, Computed Rotor Unbalance, LP Turbine Midspan Balance Plane.

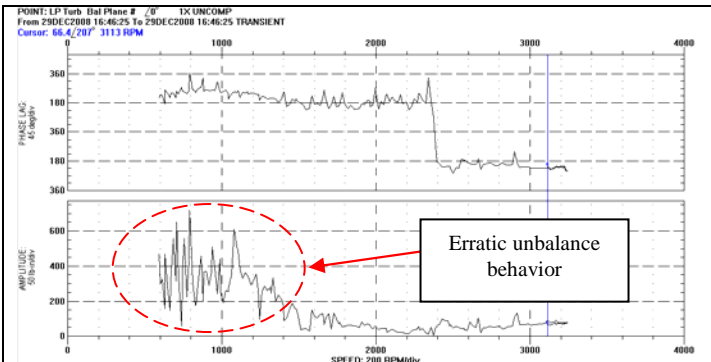


Figure 11: Bode Plot, Rotor Unbalance, LP Turbine Bearing #3 Balance Plane.

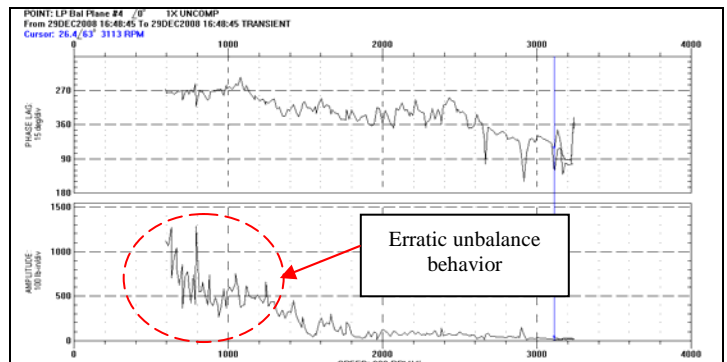


Figure 13: Bode Plot, Computed Rotor Unbalance, LP Turbine Bearing #4 Balance Plane.

The unbalance distributions clearly showed erratic behavior (rapid changes in unbalance distribution) below the first balance resonance of the LP turbine rotor from 1000 rpm to 1600 rpm (compare green dotted circle areas to red dotted circle areas in figures 9 through 15). Since the rotor mass distribution should not change that rapidly, the rotor or bearing stiffness could be changing. Likewise, it is very unlikely that the bearing stiffness would vary in that fashion; therefore rotor stiffness variation (asymmetrical shaft stiffness) would be a probable cause<sup>1</sup>. LP blade loss could cause a rapid change in unbalance distribution; however the change would be a step change in amplitude, phase or both, and change would not vary from run-to-run. The computed unbalance distributions suggested that a shaft crack might be present in the LP rotor based upon vibration measurements and analytical model findings.

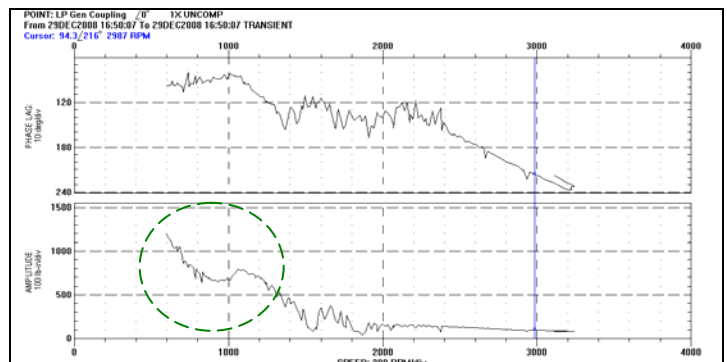


Figure 14: Bode Plot, Computed Rotor Unbalance, LP-Generator Balance Plane.

<sup>1</sup> Bently, D. E., Hatch, C. T., "Fundamentals of Rotating Machinery Diagnostics", 2002, pg. 517-533.

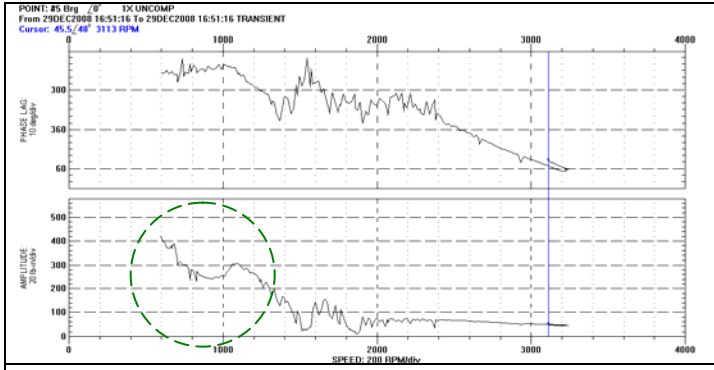


Figure 15: Bode Plot, Computed Rotor Unbalance, Generator Bearing #5 Balance Plane.

1400 cpm natural frequency, figure 19. A kink in the mode shape is apparent at the crack location.

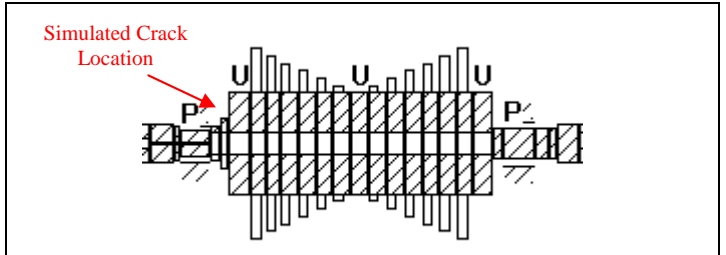


Figure 17: LP Turbine Portion of Rotor Model, Simulated Crack Location Indicated by Red Arrow.

Vibration data, slow roll measurements, balance corrections, and unbalance distribution computations all clearly pointed to a shaft crack in the LP rotor, suggesting that it might be in the vicinity of bearing #4 (generator end). However, inspection findings revealed that the crack was near bearing #3 (HP turbine end). Why were vibration levels higher at bearing #4 when the crack was near bearing #3?

The rotor dynamics model provides an answer to this question. Effects of a shaft crack near bearing #3 can be simulated using the rotor model. Natural frequencies and mode shapes of the rotor were computed with and without a crack present at approximately the location of the actual crack. Simulating a crack means reducing the diameter of rotor elements at the crack location, thereby reducing the bending stiffness of the shaft. Without the crack, amplitudes of the rotor mode shape at 3600 rpm were approximately equal at both ends of the LP turbine, see figure 16.

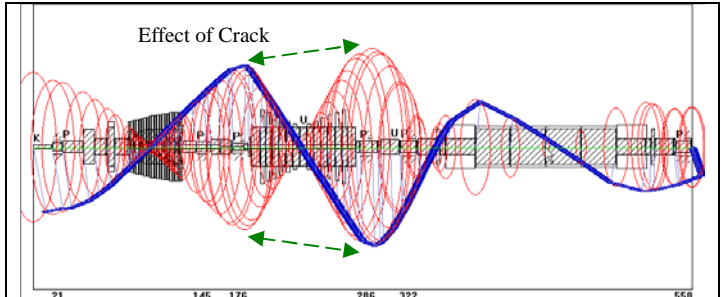


Figure 18: Mode shape at 3600 rpm with simulated shaft crack at HP End of LP Turbine.

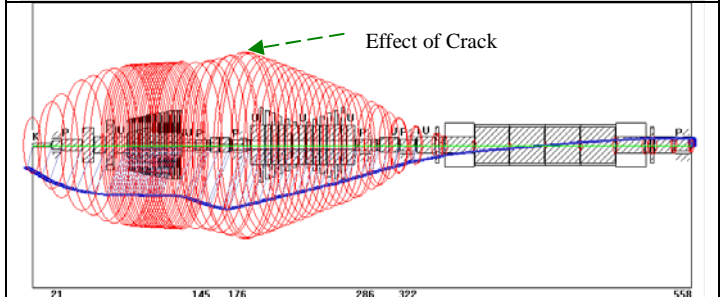
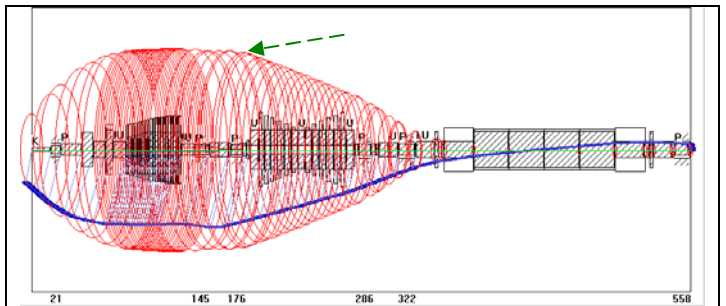


Figure 19: Mode Shape at 1400 cpm (rpm), Rotor First Natural Frequency, without crack (top), with HP End LP turbine shaft crack (bottom).

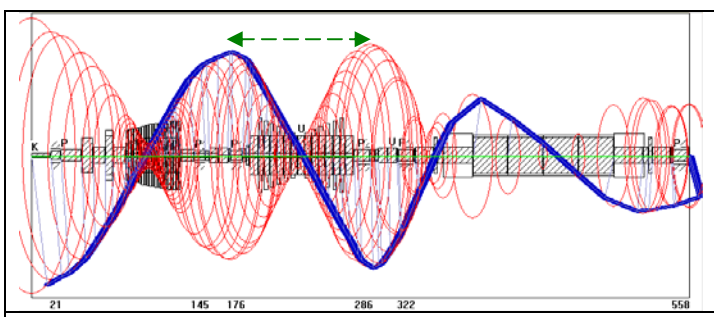


Figure 16: Mode shape at 3600 rpm without simulated shaft crack.

Next, a simulated crack was introduced into the model by reducing the cross section area of the rotor element by 50% near the actual crack location, see figure 17. Rotor model natural frequencies and mode shapes were recomputed with the simulated crack. At 3600 rpm, the mode shape clearly shows that the amplitude at the generator end of the LP rotor is greater than the amplitude at the HP turbine end, figure 18. The effects of the cracked shaft were also evident in the mode shapes at the

An obvious question would be: Would a similar mode shape change occur if the crack were at the generator end of the LP turbine? A similar crack was also simulated at the other end of the LP rotor, figure 20. The mode shape at 3600 rpm showed



an increase in amplitude at the HP end of the rotor compared to the generator end when the crack was located at the generator end of the rotor. This behavior is generally not intuitively obvious, however the model does explain observed vibration symptoms.

## SUMMARY

The above case history shows that integration of vibration data with rotor dynamic modeling can be used to predict unbalance mass distributions and explain unusual shaft crack behavior. The initial diagnosis of shaft crack was shown to be correct; however location of the crack did not immediately correspond with vibration measurements. Integration of rotor dynamic model and vibration measurements were used to generate mass distributions which accurately explained balance response of the rotor and the location of the shaft crack. Initially, rotor dynamic modeling focused upon simulating a rotor crack near bearing #4. However, computed mode shapes of the rotor with the simulated crack at that location did not match observed vibration symptoms. Further simulations revealed that the proper location of the simulated crack should be near bearing #4. These computed results matched the observed vibration symptoms and correlated very well with the actual location of the crack. In short, due to the modal response of this LP rotor system, vibration symptoms of a cracked shaft should be used to investigate the occurrence of shaft crack at an axial symmetric location from where the vibration data logically indicates. Fortunately, a significant cost savings occurred by avoiding catastrophic shaft crack failure of this rotor. The economic impact of the potential cracked shaft failure while in service was estimated as \$4,930,000 (\$6,900,000 in 2008 dollars).

## REFERENCES

Bently, D. E., Hatch, C. T., "Fundamentals of Rotating Machinery Diagnostics", 2002, pg. 1

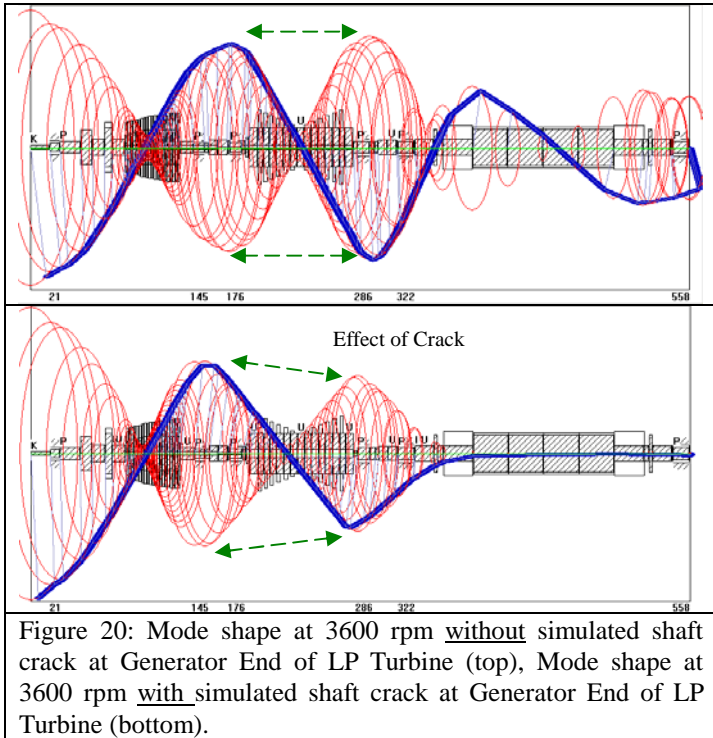


Figure 20: Mode shape at 3600 rpm without simulated shaft crack at Generator End of LP Turbine (top), Mode shape at 3600 rpm with simulated shaft crack at Generator End of LP Turbine (bottom).

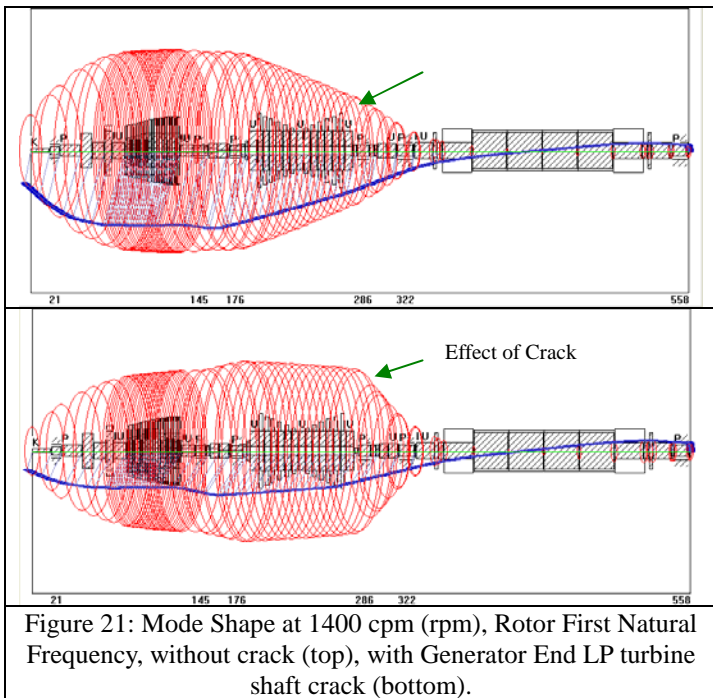


Figure 21: Mode Shape at 1400 cpm (rpm), Rotor First Natural Frequency, without crack (top), with Generator End LP turbine shaft crack (bottom).